Wall-drag effect on diffusion of colloidal particles near surfaces: A photon correlation study

M. I. M. Feitosa and O. N. Mesquita*
Departamento de Fisica, Universidade Federal de Minas Gerais, Belo Horizonte, 31270 Minas Gerais, Brazil
(Received 13 May 1991)

The reduction of the diffusion coefficient of latex spheres near glass surfaces was measured by photon correlation spectroscopy. Theory and experiment are not in agreement; possible causes for the discrepancy are discussed. In addition, the diffusion coefficient of sedimented latex spheres on a glass surface decreases with decreasing Debye length of the solution. This shows that the mean particle-surface separation distance decreases as the strength of the double-layer repulsion between the latex spheres and the glass surface is weakened. The utility of photon correlation spectroscopy for studies of interactions between colloidal particles and surfaces is discussed.

PACS number(s): 68.45.−v, 05.40.+j, 82.65.−i

I. INTRODUCTION

Our interest in the study of Brownian motion of large particles near surfaces was initially motivated by recent photon correlation experiments at growing crystal-melt interfaces [1]. One of the models to explain the anomalously large light scattering observed at the boundary layer of liquid adjacent to the growing fronts was based on the diffusion of gaseous microbubbles near the crystal surfaces [2]. However, a better understanding of diffusion of large particles near surfaces is needed. Photon correlation spectroscopy can be used to measure the diffusion coefficient of the diffusing particles. If the motion is in the bulk liquid, the well-known Einstein-Stokes equation for free diffusion of spherical particles can be used to obtain the particle sizes from the measured diffusion coefficients. However, if the particles approach a surface, the Stokes viscous force increases, resulting in a reduction of the diffusion coefficient. This "wall-drag effect" becomes important when the particle radius R is comparable with the distance of its center Z from the surface ($R/Z \approx 1$). Thus, to obtain the particle size, corrections must be introduced in the usual Einstein-Stokes relation. Lan, Ostrowsky, and Sornette [3] have studied the dynamic behavior of Brownian particles close to a glass surface by using photon correlation spectroscopy from an evanescent wave with variable penetration depth ξ. They used a water suspension of calibrated latex spheres with radius $R = 45$ nm. Surface correlation spectra strongly differed from the bulk measurements and were completely interpreted in terms of the wall's mirror effect and the evanescent wave geometry. In this experiment the wall-drag effect was neglected because $R/\xi \ll 1$. Since there are no experiments in Brownian motion near surfaces where the wall-drag effect is dominant, we have made measurements of the diffusion coefficient of calibrated latex spheres with radius $R = 1.0$ μm suspended in water as a function of their distance from the surfaces of two optical glass flats. We observed the reduction of the diffusion coefficient due to the wall-drag effect and compared the experimental results with available theories.

The forces between surfaces and colloidal particles are also important. The competition between double-layer repulsion and van der Waals attraction determines whether particles will be adsorbed onto surfaces. This is the basis of the Derjaguin-Landau-Verwey-Overbeeck (DLVO) theory of colloidal stability [4]. Recently, Prieve and collaborators [5,6] have reported remarkable experimental studies of these interactions. In these experiments, the goal was to obtain the mean particle-surface separation distance between large latex spheres suspended in water and water-glycerol solutions, and a glass surface. For a certain range of solution ionic strengths the particles remained at finite distances away from the glass surface without adsorption due to the double-layer repulsion. In Ref. [5] the instantaneous particle-surface separation distance was deduced from the measured translation speed of a large latex sphere ($R = 7.5$ μm) in linear shear flow along the surface. To obtain the relation between separation distance and translation speed, the creeping flow approximation of the hydrodynamic equations was used. In some cases, the separation distance was unexpectedly found to be dependent on the flow rate, a result which casts some doubts upon this method. In Ref. [6], Prieve, Luo, and Lanni used total internal reflection microscopy (TRIM) to determine the instantaneous separation distance between sedimented particles and a glass surface. By using an evanescent wave geometry with variable penetration depth, they restricted the scattering to particles very near the surface. The scattered intensity increased as the particles approached the surface. This technique had excellent spatial resolution, but the actual value for the particle-surface separation distance could not be obtained.

We report the use of photon correlation spectroscopy to study the double-layer repulsion between calibrated latex spheres ($R = 1.0$ μm) and a glass surface. The mean particle-surface separation distance was obtained by measuring the reduction of the diffusion coefficient due to the wall-drag effect for solutions with different ionic strengths. Our method is experimentally simpler than the previous methods and the creeping motion approximation is more suited to our case. The drawbacks of our

method are the following: (1) We cannot obtain from the measurements the particle potential-energy profile. Actually, we have to model it to extract the particle-surface separation distances from diffusion measurements. (2) At present, there is no exact analytical solution for the intensity-time autocorrelation function of the scattered light by Brownian particles when the wall-drag effect is included. In order to analyze the data, we had to use an approximate solution for the correlation function.

In spite of the limitations of the method described in this paper, we believe this work opens up new possibilities for the theoretical and experimental study of Brownian motion and interactions between colloidal particles and surfaces.

II. THEORETICAL BACKGROUND ON DIFFUSION

A. Free diffusion

Let us consider a spherical particle of radius R executing Brownian motion in a liquid of viscosity η. The particle of interest is far from any surface. By "far" we mean that the particle-surface separation distance Z is very large compared with R ($R/Z \ll 1$). The motion of the particle is described by the diffusion equation [7]

$$\frac{\partial P(\mathbf{r},\tau|\mathbf{r}',0)}{\partial t} = D_0 \nabla^2 P(\mathbf{r},\tau|\mathbf{r}',0) , \tag{1}$$

where $P(\mathbf{r},\tau|\mathbf{r}',0)$ is the conditional probability of finding the particle at position $\mathbf{r}$ at time $t=\tau$ if at $t=0$ it was at position $\mathbf{r}'$; D_0 is the free-particle diffusion coefficient. The Stokes viscous force on the particle is given by

$$F_0 = \mu v = 6\pi\eta R v , \tag{2}$$

where v is the speed of the particle and μ is a friction coefficient. The Einstein-Stokes equation is written as

$$D_0 = \frac{k_B T}{\mu} = \frac{k_B T}{6\pi\eta R} , \tag{3}$$

where k_B is Boltzmann's constant and T is the absolute temperature. A solution to Eq. (1) can be written as

$$P(\mathbf{r},\tau|\mathbf{r}',0) = \frac{\exp(-|\mathbf{r}-\mathbf{r}'|^2/4D_0\tau)}{(4\pi D_0\tau)^{3/2}} , \quad \tau \geq 0 . \tag{4}$$

B. The wall's mirror effect

Let us consider the Brownian motion of a very small particle near a reflecting plane surface placed at $Z=0$. If the particle is sufficiently small such that the change in its diffusion coefficient occurs in a very thin boundary layer adjacent to the surface, and can be neglected in the overall motion, the only effect due to the wall is to break the translation symmetry of the problem. The motion of the particle is described by the same equation (1) but with reflection boundary conditions at $Z=0$, then [7]

$$P(\mathbf{r},\tau|\mathbf{r}',0) = \frac{\exp(-|\mathbf{r}_\parallel-\mathbf{r}'_\parallel|^2/4D_0\tau)}{(4\pi D_0\tau)^{3/2}} \times \left[\exp\left[-\frac{(Z-Z')^2}{4D_0\tau} \right] + \exp\left[-\frac{(Z+Z')^2}{4D_0\tau} \right] \right] , \quad \tau \geq 0 \tag{5}$$

where $\mathbf{r}_\parallel$ and $\mathbf{r}'_\parallel$ are the particle position coordinates in the x-y plane parallel to the surface, and Z and Z' are the coordinates normal to the surface.

C. The wall-drag effect

Let us consider now the Brownian motion of a large particle near a reflecting surface. In addition to the wall's mirror effect described in Sec. II B, we have to take into account the change in diffusion coefficient due to the wall-drag effect as the particle approaches the surface. In order to determine the change in diffusion coefficient, one has to determine the change in the Stokes viscous force. This problem has an old history initiating with Lorentz in 1907 and Faxen in 1927, as mentioned in a more recent paper by Brenner [8]. Brenner undertook the calculation of the Stokes viscous force $F_{S\perp}$ for a spherical particle moving normal to a flat surface. Using the creeping-flow approximation for the hydrodynamic equations he obtained

$$F_{S\perp} = F_0 \lambda_\perp , \tag{6}$$

where

$$\lambda_\perp = \tfrac{4}{3}\sinh\alpha \times \sum_{n=1}^{\infty} \frac{n(n+1)}{(2n-1)(2n+3)} \times \left[\frac{2\sinh[(2n+1)\alpha] + (2n+1)\sinh(2\alpha)}{4\sinh^2[(n+\frac{1}{2})\alpha] - (2n+1)^2\sinh^2\alpha} - 1 \right] , \tag{7}$$

with $\alpha = \cosh^{-1}(Z/R)$, where as before R is the particle radius and Z is the distance from its center to a surface. The complicated expression (7) can be replaced by a simpler one,

$$\lambda_\perp = 1 + \frac{R}{S} , \tag{8}$$

where $S = Z - R$. for $S/R \geq 0.1$ the error made when we use Eq. (8) is around 5% and decreases as S/R increases.

Goldman, Cox, and Brenner [9] have discussed the problem of the Stokes viscous force $F_{S\parallel}$ on a spherical particle moving parallel to a flat surface. They made a comparison between two approximate analytical solutions and an exact numerical solution. In the region $S/R \geq 0.04$ the approximate solution by Faxen gives good results, with errors smaller than 5%. Faxen's solution can be written as

$$F_{S\parallel} = F_0 \lambda_\parallel , \tag{9}$$

where

$$\lambda_{\parallel}=\left[1-\frac{9}{16}\left[\frac{R}{Z}\right]+\frac{1}{8}\left[\frac{R}{Z}\right]^3-\frac{45}{256}\left[\frac{R}{Z}\right]^4-\frac{1}{16}\left[\frac{R}{Z}\right]^5\right]^{-1} . \quad (10)$$

The diffusion coefficient of a particle near a surface can then be written as

$$D_{\perp}=\frac{D_0}{\lambda_{\perp}} \text{ and } D_{\parallel}=\frac{D_0}{\lambda_{\parallel}} . \quad (11)$$

Besides the reduction effect, the diffusion coefficient becomes anisotropic as the particle approaches a surface ($D_{\perp}\neq D_{\parallel}$). The problem now is to calculate $P(\mathbf{r},\tau|\mathbf{r}',0)$ with a reflecting wall at $Z=0$ and the wall-drag effect included. The equation for $P(\mathbf{r},\tau|\mathbf{r}',0)$ then reads

$$\frac{\partial P}{\partial t}=D_{\parallel}(Z)\left[\frac{\partial^2 P}{\partial x^2}+\frac{\partial^2 P}{\partial y^2}\right]+D_{\perp}(Z)\frac{\partial^2 P}{\partial Z^2}+\frac{\partial D_{\perp}(Z)}{\partial Z}\frac{\partial P}{\partial Z} . \quad (12)$$

This equation is not trivial to solve, and we shall pursue an approximate solution in the next section.

III. TIME AUTOCORRELATION FUNCTION OF THE SCATTERED LIGHT BY BROWNIAN PARTICLES

With the technique of photon correlation spectroscopy in a homodine detection scheme, one measures the time autocorrelation function of the scattered light intensity $\langle I(t)I(t+\tau)\rangle$. For a review on this subject see Refs. [10] and [11]. For light scattered by many independent Brownian particles one can write

$$g^{(2)}(\tau)=\frac{\langle I(t)I(t+\tau)\rangle}{\langle I(t)\rangle^2}=1+|g^{(1)}(\tau)|^2 \quad (13)$$

and

$$g^{(1)}(\tau)=\frac{e^{-i\omega_0\tau}}{|E_i|^2}\int_v\int_v E_i(\mathbf{r})E_i(\mathbf{r}')e^{i\mathbf{q}\cdot(\mathbf{r}-\mathbf{r}')}\times P(\mathbf{r},\tau|\mathbf{r}',0)d\mathbf{r}d\mathbf{r}' , \quad (14)$$

where ω_0 is the frequency of the incident light, $E_i(\mathbf{r})$ and $E_i(\mathbf{r}')$ are the field amplitudes of the incident light for a single polarization at positions r and r', and $\mathbf{q}$ is the scattering wave vector. If the scattering volume is uniformly illuminated one has

$$g^{(1)}(\tau)=e^{-i\omega_0\tau}\int\int e^{i\mathbf{q}\cdot(\mathbf{r}'-\mathbf{r})}P(\mathbf{r},\tau|\mathbf{r}',0)d\mathbf{r}d\mathbf{r}' . \quad (15)$$

A. Free diffusion

For free diffusion and uniform illumination one can use Eqs. (4), (15), and (13) to obtain

$$g^{(1)}(\tau)=e^{-i\omega_0\tau}e^{-q^2D_0\tau}$$

and

$$g^{(2)}(\tau)=1+e^{-2q^2D_0\tau} . \quad (16)$$

If particles of different sizes are present there is a distribution of diffusion coefficients. In this case $g^2(\tau)$ is not a single exponential but a superpositon of exponentials. One of the methods to analyze such a correlation function is the method of cumulants [10,11], where

$$\ln[g^{(2)}(\tau)-1]=\sum_{m=1}^{\infty}\frac{k_m(-\tau)^m}{m!} .$$

For a single exponential only the first cumulant $k_1=2q^2D_0$ is different from zero. In most practical situations we only keep the first two terms of the expansion above. The ratio k_2/k_1^2 is called polydispersity and gives an estimate of the width of the diffusion coefficient distribution. The polydispersity is a measure of how far the correlation function is from a single exponential.

B. The wall's mirror effect

Lan, Ostrowsky, and Sornette [3] have calculated $g^{(1)}(\tau)$ considering the wall's mirror effect with an evanescent wave geometry. In that case $E_i(\mathbf{r})=E_0e^{-r/\xi}$ and $E_i(\mathbf{r}')=E_0e^{-r'/\xi}$, where ξ is the penetration depth of the evanescent wave. They obtained

$$g^{(1)}(\tau)=e^{-i\omega_0\tau}e^{-q_{\parallel}^2D_0\tau}\times\left[\mathrm{Re}[e^{f^2}\mathrm{erfc}(f)]-\frac{1}{q_{\perp}\xi}\mathrm{Im}[e^{f^2}\mathrm{erfc}(f)]\right] ,$$

with $f=[(D_0\tau)^{1/2}/\xi](1+iq_{\perp}\xi)$, where $q_{\parallel}$ and $q_{\perp}$ are the scattering wave vectors parallel and normal to the surface. If $q_{\perp}=0$, $|g^{(1)}(\tau)|=e^{-q_{\parallel}^2D_0\tau}$. If $\xi\gg(D_0\tau)^{1/2}$ then $|g^{(1)}(\tau)|=e^{-q^2D_0\tau}$. In both cases the free diffusion single-exponential behavior is obtained and the wall's mirror effect is lost. Therefore, if we want to isolate out the wall-drag effect from the wall's mirror effect it is sufficient to work with $q_{\perp}=0$ or with uniform illumination in a sample whose thickness is much larger than $(D_0\tau)^{1/2}$.

C. The wall-drag effect

To obtain $g^{(1)}(\tau)$ including the wall-drag effect, one has to calculate $P(\mathbf{r},\tau|\mathbf{r}',0)$ from Eq. (12), plug the result into Eq. (15), and solve the integral equation, which is a formidable task. In our experiments we have observed that the correlation functions were most of the time reasonable single exponentials with polydispersities about 30% or less for large scattering angles ($\theta\geq 90°$). These results encouraged us to write a zero-order approximation for the correlation function as

$$g^{(2)}(\tau)\cong 1+\exp(-2q_{\parallel}^2\langle D_{\parallel}\rangle\tau-2q_{\perp}^2\langle D_{\perp}\rangle\tau+k_2\tau^2) , \quad (17)$$

where

$$\langle D_{\parallel} \rangle = \int_0^{\infty} P(Z) D_{\parallel}(Z) dZ \ ,$$
$$\langle D_{\perp} \rangle = \int_0^{\infty} P(z) D_{\perp}(Z) dZ \ , \tag{18}$$

with $P(Z)$ the normalized equilibrium distribution of particle positions along the direction normal to the surface. What is behind our approximation is that we have a great number of particles distributed along Z. In a short time interval we can think that each of these particles executes Brownian motion around different positions Z', such that during this motion the diffusion coefficients $D_{\parallel}(Z')$ remain constant. This approximation is better for larger scattering angles where the relaxation time of the correlation function is shorter, such that during this time the particles move very little around Z'. Therefore we approximate Eq. (12) for motion around Z' as

$$\frac{\partial P}{\partial t} = D_{\parallel}(Z') \left[\frac{\partial^2 P}{\partial x^2} + \frac{\partial^2 P}{\partial y^2} \right] + D_{\perp}(Z') \frac{\partial^2 P}{\partial Z^2}$$

and as a consequence

$$g^{(2)}(\tau, Z') = 1 + \exp[-2q_{\parallel}^2 D_{\parallel}(Z')\tau - 2q_{\perp}^2 D_{\perp}(Z')\tau] \ ,$$

and finally,

$$g^{(2)}(\tau) = \int_0^{\infty} P(Z') g^{(2)}(\tau, Z') dZ' \ .$$

We can then make a cumulant analysis of $g^{(2)}(\tau)$ above to obtain Eq. (17). For $q_{\perp}=0$ the polydispersity $\mathcal{P}$ in this approximation is given by $\mathcal{P}=(\langle D_{\parallel}^2 \rangle - \langle D_{\parallel} \rangle^2)/\langle D_{\parallel} \rangle^2$ and for $q_{\parallel}=0$, $\mathcal{P}=(\langle D_{\perp}^2 \rangle - \langle D_{\perp} \rangle^2)/\langle D_{\perp} \rangle^2$. From numerical estimates based on this approximation applied to our experiments we expect polydispersities of at most 5%.

IV. DOUBLE-LAYER REPULSION

Let us consider the interaction between equal-sign large charged particles in an electrolyte. The presence of mobile ions in the solution weakens the Coulomb repulsion by a process known as Debye screening. Ions of opposite charge form a diffuse cloud around the surface of the charged particles, which has a net charge equal and opposite to that of the surface. The thickness of this cloud is called the Debye length L_D, and is given by [4],

$$L_D = \left[\frac{\epsilon k_b T}{2e^2 n_0} \right]^{1/2} , \tag{19}$$

where ϵ is the dielectric constant of the solution, n_0 is the ionic strength, e is the proton charge, and $k_B T$ is the thermal energy. This diffuse cloud together with the layer of fixed charges on the particle's surface is called the double layer. The Coulomb repulsion acts between two particles if their double layer overlaps. As one increases the ionic strength, L_D decreases, then the particles can get closer. If they approach sufficiently for the van der Waals attraction to act, aggregation may occur. Typically L_D can vary from 1 nm in physiological saline up to about 1 μm in deionized water [5]. The same effect can occur between charged particles and charged surfaces. If L_D decreases, particles may be adsorbed onto surfaces. We can estimate the double-layer potential energy between a spherical particle and a flat surface using the Derjaguin approximation [6]:

$$U_{\mathrm{DL}}(S) = A e^{-S/L_D} \ ,$$

where $S=Z-R$, with Z the distance from the center of that particle to the surface and R the particle's radius. A is a constant that depends on the surface potentials. If the gravitational field is normal to the surface one can write the gravitational potential energy as $U_G(S)=GS$, with $G=\frac{4}{3}\pi R^3 \Delta\rho g$, where g is the acceleration of gravity, $\Delta\rho=\rho_P-\rho_L$, where ρ_P is the particle density and ρ_L is the liquid density. Thus the total potential-energy profile of sedimented charged particles on an equal-sign charged surface is

$$P(S) = C e^{-[U_{\mathrm{DL}}(S)+U_G(S)]/k_B T} \ ,$$

where C is a normalization constant. There is an equilibrium position S_0 such that $(d/dS)[U_{\mathrm{LD}}(S) + U_G(S)]_{S_0}=0$. If we write $P(S)$ in terms of S_0 one has

$$P(S,S_0) = C e^{-(GL_D e^{-(S-S_0)/L_D} + GS)/k_b T} \ . \tag{20}$$

$P(S,S_0)$ gives the probability of finding a particle at position S. For typical L_D, $P(S,S_0)$ decays very abruptly for $S<S_0$. In this case we can think that there is a reflecting wall at S_0. In this approximate analysis we have neglected the van der Waals force, which may become important for very small particle-surface separation distances.

V. EXPERIMENT

A. Sample preparation and experimental setup

All experiments are performed with deionized water suspensions of calibrated latex spheres ($R=1.0$ μm) from Duke Scientific Co. Ionic strengths are varied by adding small amounts of NaCl to the solutions. In the various experiments the solutions are squeezed between two right-angle glass prisms, forming thin films. The prisms have optically polished surfaces with sides of 3 cm, and the separation between them is determined by mica spacers. The concentration of latex spheres is such that if in a given experiment all the spheres come to form a monolayer, the average separation distance between them is always larger than 16 μm. This assures that interactions between the spheres are negligible. The prisms were carefully cleaned in a sequence of baths: ultrasonic, trichloroethylene, acetone, and ethanol; all chemical compounds were spectroscopic grade. The working solution is placed between the prisms inside of a clean plexiglas box with a positive pressure of pure argon. Only after clamping the prisms together is the sample taken out of the clean box. This procedure is very important to avoid dust particles and to have reproducible surface conditions. To prevent evaporation of the solution film, the region of contact between the prisms is sealed around with

heated beeswax.

Our light-scattering setup is standard for photon correlation spectroscopy [10,11]. We used a He-Ne laser of 1 mW made by Opto-Eletrônica–São Carlos (Brazil), and a correlator made by Brookhaven Instruments Co. (model BI2030). The collection optics consists of two pinholes ($P_1=2$ mm and $P_2=200$ μm) and focusing lens L ($f=20$ cm), to illuminate the photomultiplier (RCA-C31034176) under a coherence area. The optical system and sample are mounted on a homemade vibration isolating table. The whole system was checked against vibrations and the sizes of latex spheres of diameter 85 nm were measured by photon correlation, for comparison purposes. The measured radius agreed with the factory value within 8%. An additional difficulty arises when we perform light scattering near surfaces. In our case, since the indices of refraction of the glass and water are different (1.50 and 1.33), high-quality optical surfaces are needed to avoid static scattering at the glass-solution interfaces. In order to guarantee a homodine detection scheme, we mapped out the intensity scattered statically by different regions of the glass-water interface without the latex spheres. The intensities measured were always about ten times smaller than the scattered intensity by the solution with the spheres. This residual static scattering caused a slight increase in the polydispersity of the correlation functions. As mentioned before, $g^{(2)}(\tau)$ is the quantity measured in the homodine configuration. The scattering wave vector is $\mathbf{q}=\mathbf{k}_0-\mathbf{k}_S$, where $\mathbf{k}_0$ and $\mathbf{k}_S$ are the incident and scattered light wave vectors, respectively. For quasielastic scattering $|\mathbf{k}_0|\cong|\mathbf{k}_S|$, then, $q=2k_0\sin(\theta/2)$, where θ (the scattering angle) is the angle between $\mathbf{k}_0$ and $\mathbf{k}_S$.

B. Measurements of the diffusion coefficient with gravity g parallel to the surfaces

The experimental scheme used is shown in Fig. 1. The working solution was placed between the two prisms, which were clamped together with a mica spacer at one end. The other ends of the prisms were kept in close contact. This wedged gap with the solution was important, because it allowed us to vary continuously the separation distance h between the glass surfaces by moving the whole system up and down without changing the optical alignment. The vertical motion was provided by a precision stage attached to the prisms, such that the vertical readings of the stage micrometer could be converted to separation distance h between the glass surfaces. Typically a vertical displacement of 1 mm corresponded to a variation in h of 0.8 μm. The error in vertical readings was of 5 μm, resulting in a negligible error in h of 0.004 μm. The thickness of the mica spacers was measured with a Mytutoyo digital micrometer with precision of ±0.5 μm. Typically we used spacers of 20 μm, and the error in the measured thickness was about 5%. The width of the laser beam at the surface was always smaller than 300 μm. The variation of h along the beam was at most 0.24 μm. The smallest h used in our experiments was around $h=4$ μm. The overall error was 10% for the smallest h and decreased as h increased. In Fig. 1 we show (a) the detail of the wedged gap with the solution, (b) the scattering geometry, and (c) the scattering wave vector parallel to the surfaces.

The measured correlation functions were analyzed by the method of cumulants. Since $q_\perp=0$ in these experiments, from the first cumulant one obtains the value for $\langle D_\parallel\rangle$. The polydispersities varied from 10% up to 30%, with no clear correlation with h. Since $D_0=2.2\times10^{-9}$ cm^2/s we can obtain $\langle\lambda_\parallel^{-1}\rangle=\langle D_\parallel\rangle/D_0$. A plot of $\langle\lambda_\parallel^{-1}\rangle$ as a function of h is shown in Fig. 2. The dots are the experimental data and correspond to measurements in the same run. Different runs presented essentially the same results. In Sec. II C we developed the theory of the wall-drag effect for colloidal particles near a single surface. In our experiments we have the particles between two surfaces. We will assume that the corrections to the

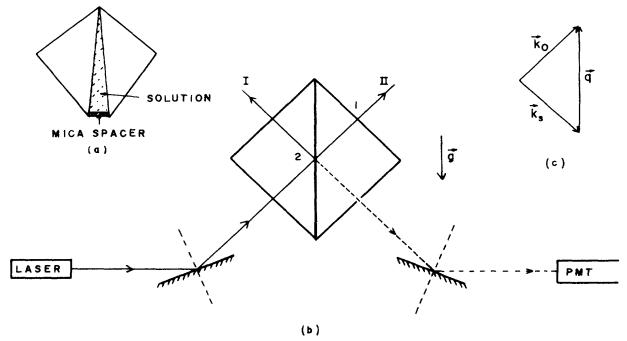

FIG. 1. Experimental geometry for measurements of the diffusion coefficient of latex spheres between two glass surfaces with gravity **g** parallel to the surfaces. (a) Detail of the wedged gap with a solution; (b) scattering geometry; (c) scattering wave vector **q** parallel to the surfaces.

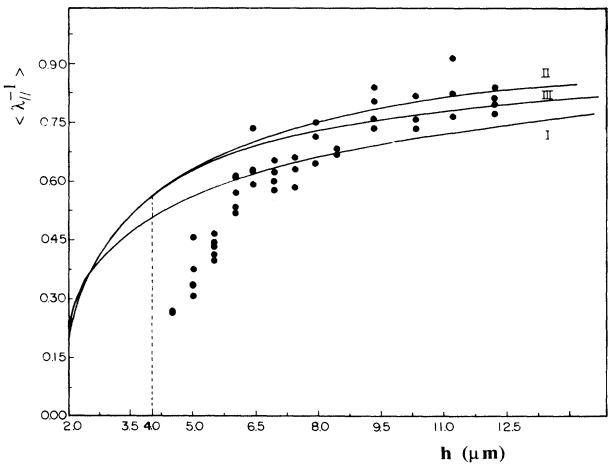

FIG. 2. Dots are experimental data of the ratio $\langle\lambda_\parallel^{-1}\rangle$ between the parallel diffusion coefficient near the surfaces and the free diffusion coefficient of latex spheres as a function of the separation distance h between the glass surface for measurements with gravity **g** parallel to the surfaces. Theoretical curves I, II, and III are described in the text.

Stokes force due to each surface can be added linearly. Correction in the viscous Stokes force caused by surface 1 can be written as $\Delta_1=F_0\lambda_1-F_0=F_0(\lambda_1-1)$; correction due to surface 2 can be written as $\Delta_2=F_0(\lambda_2-1)$. The total correction will be $\Delta=\Delta_1+\Delta_2=F_0(\lambda_{\text{eff}}-1)$, then $\lambda_{\text{eff}}=\lambda_1+\lambda_2-1$. If the distance of the center of a particle from surface 1 is Z, its distance from surface 2 is $h-Z$. Then

$$\lambda_{\text{eff}}=\lambda\left[\frac{R}{Z}\right]+\lambda\left[\frac{R}{h-Z}\right]-1\ , \tag{21}$$

with λ given by Eq. (8) or (10). Our measurements must then be compared with

$$\langle\lambda_{\parallel}^{-1}\rangle=\int_0^{\infty}P(Z)\lambda_{\parallel\text{eff}}^{-1}dZ\ . \tag{22}$$

The linear superposition used is expected to give better results for larger hs. For smaller hs, hydrodynamic interactions between surface 1 and surface 2 mediated by the motion of the particle can be important, thus this approximation should become worse. For comparison, let us consider the result of Faxen [8], who calculated $\lambda_{\parallel}$ for a sphere between two flat surfaces when $R/Z\ll 1$. When the particle is at the middle distance between the two surfaces $(h/2)$, Faxen's complete solution gives $\lambda_{\parallel}=1+1.004R/(h/2)$, whereas our linear superposition gives $\lambda_{\parallel}=1+1.125R/(h/2)$. The two solutions are reasonably close, indicating that our approximation is not too bad.

The theoretical curves I, II, and III indicated in Fig. 2 were obtained from Eqs. (21), (10), and (22) for different distributions $P(Z)$. In curve I the particles were assumed uniformly distributed along the solution. Therefore,

$$P_{\text{I}}(Z)=\begin{cases}(h-2R)^{-1}\ , & R\le Z\le h-R\\ 0\ \text{ otherwise }\ Z\ .\end{cases}$$

In curve II the particles were assumed to be centered between the surfaces; therefore $P_{\text{II}}(Z)=\delta(Z-h/2)$.

In curve III the particles were assumed uniformly distributed in the solution, but remained at position $S_0=1$ μm away from the surfaces for $h>4$ μm and at the middle of the solution for $h\le 4$ μm. Therefore, for $h>4$ μm,

$$P_{\text{III}}(Z)=\begin{cases}(h-2R-2S_0)^{-1}\ , & R+S_0\le Z\le h-R-S_0\\ 0\ \text{ otherwise } Z,\end{cases}$$

and $P_{\text{III}}(Z)=\delta(Z-h/2)$ for $h\le 4$ μm. The assumptions behind curves II and III is that there is a strong repulsion between the particles and surfaces: in curve II this repulsion is of long range and in curve III this repulsion acts up to a distance of 1 μm from the surfaces. If we look at the data for large hs, we cannot decide between curves II or III, but we can say that the particles remain at least 1 μm away from the surfaces. This distance (1 μm) is of the order of the Debye length for deionized water, similar to the one used in our experiments. We will show later that, in fact, the particles remain away from the glass surfaces without adsorption due to the double-layer repulsion. For small values of h the discrepancy between all theoretical curves and the experimental data is apparent. This discrepancy may be due to a failure of the superposition principle, and then may be of purely hydrodynamic character. We note, however, that at least in the region $R/Z\ll 1$, Faxen's complete solution results in smaller viscous forces than those given by our linear superposition approximation, which would increase the discrepancy between our experimental data and theory for smaller values of h. In addition, we cannot disregard the possibility of an additional friction due to electrical interactions between the particles, the electrolyte, and the glass surfaces [12]. If the scattered light is collected along the direction of the reflected beam indicated in Fig. 1, the scattering wave vector would be normal to the surfaces and then we could measure $\langle\lambda_{\perp}^{-1}\rangle$. Even though we tilt the prisms slightly to avoid the reflected beam to enter directly into the collection optics, a large amount of forward scattering reflected at the second surface will be collected together with the light of interest. Then we have a mixture of light scattered at angle θ and $\pi-\theta$. As a result the correlation functions are highly nonexponential. In addition, at smaller scattering angles the relaxation times of the correlation functions are larger and our approximation that $D_{\parallel}(Z)$ and $D_{\perp}(z)$ are constant during this time becomes worse. As a rule, when a geometry is good for measuring $D_{\perp}$ it is bad for measuring $D_{\parallel}$ and vice versa.

C. Measurements of the diffusion coefficient with gravity g normal to the surfaces

In this experiment we were mainly interested in observing sedimentation effects. The geometry used is shown in Fig. 3. If we use laser 2, $(q_{\perp}/q_{\parallel})^2\cong 6$, therefore the decay time of the correlation function is dominated by $q_{\perp}^2\langle D_{\perp}\rangle$ in the region where $D_{\perp}\cong D_{\parallel}$. For laser 1, $(q_{\parallel}/q_{\perp})^2\cong 6$, then the decay time is dominated by $q_{\parallel}^2\langle D_{\parallel}\rangle$. In principle, in this way we could obtain both $\langle D_{\perp}\rangle$ and $\langle D_{\parallel}\rangle$. But due to the reasons pointed out in the last section, the measurement of $\langle D_{\parallel}\rangle$ in this geometry is very difficult to

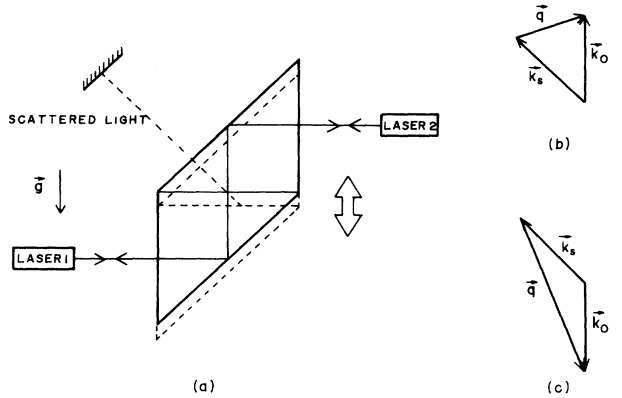

FIG. 3. Experimental geometry for measurements of the diffusion coefficient of latex spheres between two glass surfaces with gravity g normal to the surfaces. (a) Scattering geometry; (b) scattering wave vector q if laser 1 is used; (c) scattering wave vector q if laser 2 is used.

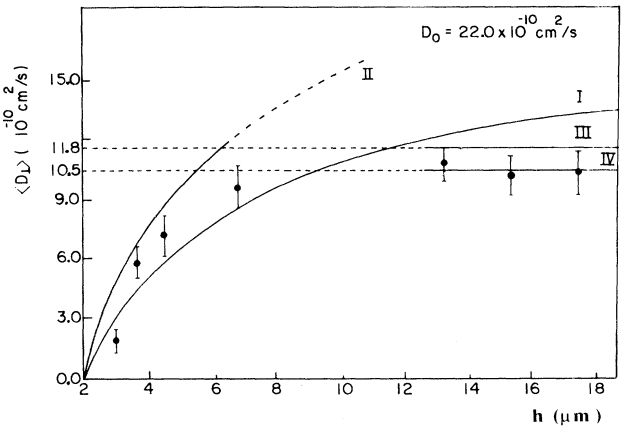

FIG. 4. Experimental data for the perpendicular diffusion coefficient $\langle D_\perp \rangle$ as a function of separation distance h between the glass surfaces. Sedimentation of the latex spheres on a glass surface is apparent, since for large values of h, $\langle D_\perp \rangle$ saturates at approximately $D_0/2$. Theoretical curves I, II, III, and IV are described in the text.

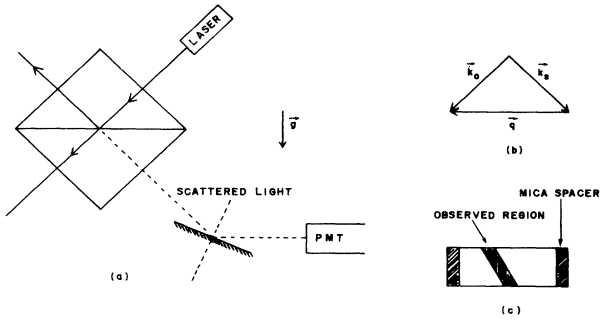

FIG. 5. Experimental geometry for measurements of particle-surface separation distances during sedimentation. (a) Scattering geometry; (b) scattering wave vector parallel to the surfaces; (c) detail of the scattering volume.

make and is not reproducible. The data shown in Fig. 4 are taken with laser 2. We then consider that the decay of the correlation function was only due to $q_\perp^2 \langle D_\perp \rangle$. This approximation becomes worse for small hs where $D_\parallel < D_\perp$. This experiment then emphasizes the importance of having pure geometries, with the scattering wave vector completely parallel or completely normal to the surfaces. The theoretical curves indicated in Fig. 4 were obtained for different $P(Z)$. In curve I the particles are assumed distributed uniformly in the solution; in curve II the particles are assumed in the middle of the solution film; curve III is the asymptotic ($h \geq 12$ μm) expression obtained with $P(Z,S_0)$ from Eq. (20) with $\Delta\rho = 0.05$ g/cm^3 and $S_0 = 0$; curve IV is the same as curve III with $\Delta\rho = 0.07$ g/cm^3 and $S_0 = 1$ μm. The effect of sedimentation is clearly seen for $h > 12$ μm, where the experimental data are well below curve I. The value $\Delta\rho = 0.05$ g/cm^3 is the accepted value for latex spheres in water. Prieve, Luo, and Lanni [6] have observed that their experimental data would agree better with theory if they had used $\Delta\rho = 0.07$ g/cm^3 rather than $\Delta\rho = 0.05$ g/cm^3. For some reason that we do not understand, the discrepancy between experiment and theory for smaller values of h for $\langle D_\perp \rangle$ was smaller than in the previous case of $\langle D_\parallel \rangle$. Perhaps the assumption that the decay time was only caused by the term $q_\perp^2 \langle D_\perp \rangle$ has introduced errors that partially canceled the errors introduced by the other approximations. The important consequence of this experiment is that it is possible to detect sedimentation by this method. In the next section, though in a different geometry, we will explore this possibility to study interfacial forces.

D. Measurements related to the double-layer repulsion

In the last two sections the effect of repulsion between the surfaces and particles as well as the effect of sedimentation were clearly demonstrated. In this section we will show that the interaction observed is due to the double-layer repulsion and that photon correlation spectroscopy can be used to study interaction forces between surfaces and colloidal particles.

To avoid the linear superposition done before when we dealt with particles between two surfaces, we used mica spacers of 200 μm, such that one glass surface was very far apart from the other. For particles sedimented on one of the surfaces the problem was then restricted to interactions between particles and a single flat surface.

We have used suspensions of latex spheres ($R = 1.0$ μm) in deionized water. To vary the ionic strength of the solution we added small amounts of NaCl in concentrations from zero up to 40 mol/m^3. In addition to NaCl, 0.5 mol/m^3 of SDS ($C_{12}H_{25}NaO_4S$) was included in the solution to inhibit sticking of particles to the glass surface.

For the concentration of SDS used we have observed some adsorption of particles on the glass surface for NaCl concentrations higher than 40 mol/m^3. The experimental geometry is shown in Fig. 5: (a) scattering geometry; (b) scattering wave vector parallel to the surfaces; (c) scattering volume. Here we do not have a

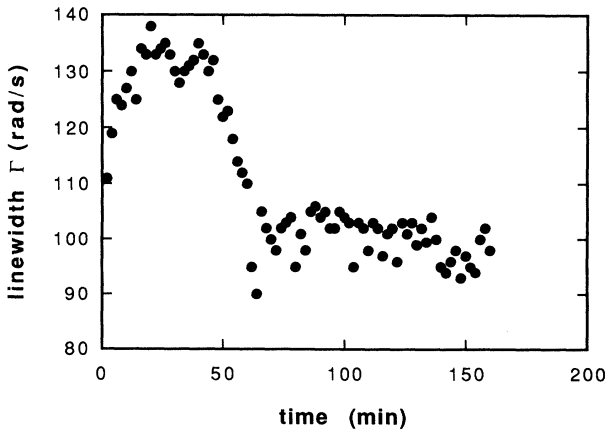

FIG. 6. Measured linewidth Γ of the light scattered by latex spheres during sedimentation as a function of the time interval after inversion of the prisms.

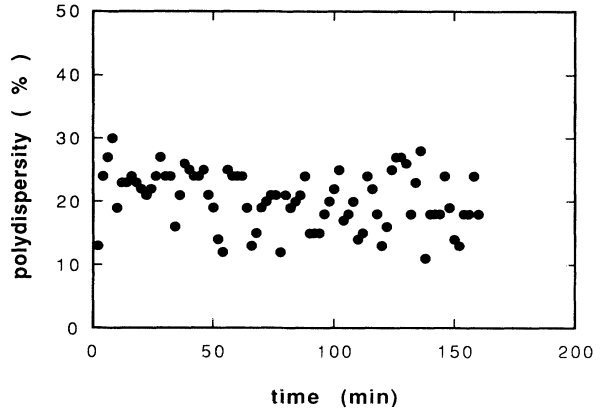

FIG. 7. Polydispersity as a function of time for the data of Fig. 6.

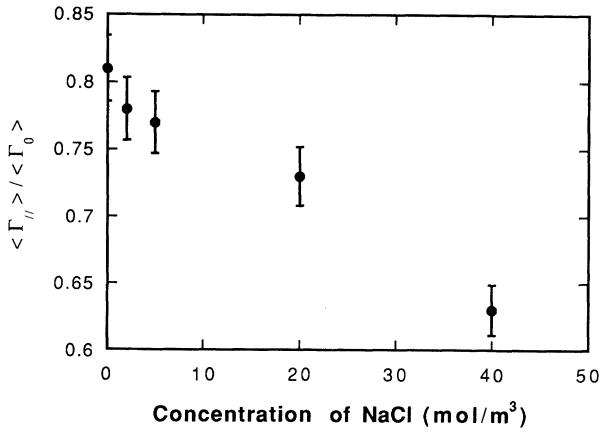

FIG. 8. Variation of $\langle\Gamma_{\parallel}\rangle/\langle\Gamma_0\rangle=\langle D_{\parallel}\rangle/\langle D_0\rangle=\langle\lambda_{\parallel}^{-1}\rangle$ as a function of the concentration of NaCl in the solution of latex spheres. The data indicate that the spheres approach the glass surface for smaller Debye lengths.

wedged gap as in the previous sections, the separation distance between the two glass surfaces being uniform and equal to 200 μm. After the solution is placed between the two prisms following the same procedure as before, we wait for about 1 h to assure that complete sedimentation has occurred. After that we invert the prisms, and the particles start to move towards the other surface. We then start to record correlation functions. The linewidth Γ increases as the particles go towards the center of the sample away from the surfaces. Since the surfaces are far enough apart, these measurements give us the bulk value for the diffusion coefficient. As the particles approach a surface, the linewidth Γ decreases until a stationary value is achieved, when most of the particles have sedimented. The variation of Γ as a function of time during sedimentation is shown in Fig. 6. The polydispersity is shown in Fig. 7. The polydispersity was always smaller than 30%, with no correlation with the separation distance between the particles and the surface. By averaging the maximum values of Γ one obtains $\langle\Gamma_0\rangle$, and by averaging the minimum values of Γ one obtains $\langle\Gamma_{\parallel}\rangle$. From the ratio $\langle\Gamma_{\parallel}\rangle/\langle\Gamma_0\rangle=\langle D_{\parallel}\rangle/\langle D_0\rangle=\langle\lambda_{\parallel}^{-1}\rangle$. We repeat the experiment by inverting the prisms again, then one can do a few runs with the same sample. The thickness of the mica spacer (200 μm) was chosen such that complete sedimentation occurred in about 1 h. The advantage of this method is that $\langle\lambda_{\parallel}^{-1}\rangle$ was obtained from a relative measurement, where we do not need to know the exact value for the scattering angle, the exact viscosity of the solution, or the exact index of refraction. We have done experiments for different concentrations of NaCl, and consequently different Debye lengths. In Fig. 8 we show the plot of $\langle\lambda_{\parallel}^{-1}\rangle$ as a function of NaCl concentration in the solution. The error bars are the standard deviation of the data from two runs (we inverted the prisms twice) and data collected from different regions of the surface after complete sedimentation. This was done for each solution with different L_D. It is clearly seen that the particles get closer to the surface as one decreases the Debye length of the solution by adding NaCl. This is a manifestation of the Debye screening of the Coulomb repulsion between the particles and surfaces due to the presence of an electrolyte. The next step is to obtain the particle-surface separation distance as a function of the Debye length. To do that we solved numerically the following integral equation by varying the value of S_0:

$$\langle\lambda_{\parallel}^{-1}\rangle_{\text{measured}}=\int_0^{\infty}\lambda_{\parallel}^{-1}(Z)P(Z,S_0)dZ\ ,$$

with $\lambda_{\parallel}^{-1}(Z)$ from Eq. (10) and $P(Z,S_0)$ from Eq. (20), replacing S by $Z-R$. In Table I we show the positions S_0 obtained as a function of the Debye length L_D for both $\Delta\rho=0.05$ and 0.07 g/cm^3 for various concentrations of NaCl. Some of the data could not be fitted adequately. This possibly indicates some partial adsorption, or

TABLE I. Average particle-surface separation distances S_0 as a function and NaCl concentration in the 0.5-mol/m^3 solution of SDS for $\Delta\rho=0.05$ and 0.07 g/cm^3.

C_{NaCl} (mol)/m^3	L_D (nm)	$\langle\lambda_{\parallel}^{-1}\rangle$	S_0 (μm) $\Delta\rho=0.05$ g/cm^3	S_0 (μm) $\Delta\rho=0.07$ g/cm^3
0	4.3	0.81	0.61	0.88
2	3.7	0.78	0.29	0.53
5	3.1	0.77	0.22	0.45
20	1.9	0.73		0.20
40	1.4	0.63		

perhaps that Faxen's solution is no longer accurate for such short distances. In addition, van der Waals forces and ionic friction, which were neglected in the present description, may be important at such small separation distances. Spatial resolution can be increased by using larger particles such that $P(Z,S_0)$ becomes much narrower.

VI. CONCLUSIONS

In the first part of this work we reported the observation by photon correlation spectroscopy of the reduction of the diffusion coefficient of colloidal particles near surfaces due to the wall-drag effect. We were able to give an interpretation of the data for large particle-surface separation distances based on known theories of the wall-drag effect. At smaller separation distances the values for $\langle D_{\parallel} \rangle$ were considerably smaller than the theoretical predictions. Possible sources for this discrepancy are the use of linear superposition for hydrodynamic interactions or other effects not considered, such as ionic friction due to electrical interactions between the colloidal particles, electrolyte, and surfaces. For reasons that we do not understand the measured values for $\langle D_{\perp} \rangle$ agreed better with the hydrodynamic theory used than those for $\langle D_{\parallel} \rangle$.

In the second part of this work we reported the use of photon correlation spectroscopy to study double-layer repulsion between colloidal particles and surfaces. The experimental results clearly show that the colloidal particles approached the glass surface as the Debye length of the solution was decreased, a manifestation of Debye screening.

As our work indicates, additional theoretical and experimental work is necessary to utilize this technique fully for further investigations of Brownian motion of colloidal particles near surfaces.

ACKNOWLEDGMENTS

We acknowledge helpful discussions with L. O. Ladeira and H. Z. Cummins. We are specially indebted to J. P. Gollub and D. Pine for critical reading of the manuscript. This work was supported by the Brazilian Agencies, Conselho Nacional de Desenvolvimento Cientifico e Tecnologico (CNPq) and Financiadora de Estudos e projetos (FINEP).

*Present address: Department of Physics, Haverford College, Haverford, PA 19041.

[1] J. H. Bilgram, H. Guttinger, and W. Kanzig, Phys. Rev. Lett. **40**, 1394 (1978); P. Boni, J. H. Bilgram, and W. Kanzig, Phys. Rev. A **28**, 2953 (1983); U. Durig, J. H. Bilgram, and W. Kanzig, Phys. Rev. B **30**, 946 (1984); O. N. Mesquita, D. G. Neal, M. Copic, and H. Z. Cummins, *ibid.* **29**, 2846 (1984); J. P. Vesenka and Y. Yeh, Phys. Rev. A **38**, 5310 (1988).

[2] H. Z. Cummins, G. Livescu, H. Chou, and M. R. Srinivasan, Solid State Commun. **60**, 857 (1986); O. N. Mesquita, L. O. Ladeira, I. Gontijo, A. G. Oliveira, and G. A. Barbosa, Phys. Rev. B **38**, 1550 (1988); J. M. Laherrere, H. Savary, R. Mellet, and J. C. Toledano, Phys. Rev. A **42**, 1142 (1990); L. Williams, M. R. Srinivasan, and H. Z. Cummins, Phys. Rev. Lett. **64**, 1526 (1990).

[3] K. H. Lan, N. Ostrowsky, and D. Sornette, Phys. Rev. Lett. **57**, 17 (1986).

[4] E. J. W. Verwey and J. Th. G. Overbeeck, *Theory of the Stability of Lyophobic Colloids* (Elsevier, New York, 1948).

[5] D. C. Prieve and B. M. Alexander, Science **231**, 1269 (1986).

[6] D. C. Prieve, F. Luo, and F. Lanni, Faraday Discuss. Chem. Soc. **83**, 297 (1987).

[7] S. Chandrasekhar, Rev. Mod. Phys. **15**, 1 (1943).

[8] H. Brenner, Chem. Eng. Sci. **16**, 242 (1961).

[9] A. J. Goldman, R. G. Cox, and H. Brenner, Chem. Eng. Sci. **22**, 637 (1967).

[10] B. J. Berne and R. Pecora, *Dynamic Light Scattering* (Wiley, New York, 1976).

[11] *Photon Corrrelation and Light Beating Spectroscopy,* edited by H. Z. Cummins and E. R Pike (Plenum, New York, 1974).

[12] H. Ohshima, T. W. Healy, and L. R. White, J. Chem. Soc. Faraday Trans. 2 **80**, 1299 (1984).